



Mapping grassland mowing events across Germany based on combined Sentinel-2 and Landsat 8 time series

Marcel Schwieder^{a,b,*}, Maximilian Wesemeyer^a, David Frantz^{a,c}, Kira Pfoch^{a,d}, Stefan Erasmi^b, Jürgen Pickert^e, Claas Nendel^{e,f,g,h}, Patrick Hostert^{a,f}

^a Geography Department, Humboldt-Universität zu Berlin, Unter den Linden 6, 10099 Berlin, Germany

^b Thünen Institute of Farm Economics, Bundesallee 63, 38116 Braunschweig, Germany

^c Earth Observation and Climate Processes, Trier University, 54286 Trier, Germany

^d Department of Forest and Wildlife Ecology, University of Wisconsin-Madison, 1630 Linden Drive, Madison, WI 53706, USA

^e Leibniz Centre for Agricultural Landscape Research (ZALF), Eberswalder Straße 84, 15374 Müncheberg, Germany

^f Integrative Research Institute on Transformations of Human-Environment Systems (IRI THESys), Humboldt-Universität zu Berlin, Unter den Linden 6, 10099 Berlin, Germany

^g Institute of Biochemistry and Biology, University of Potsdam, Am Mühlenberg 3, 14476 Potsdam, Germany

^h Global Change Research Institute, the Czech Academy of Sciences, Bělá 986/4a, 603 00 Brno, Czech Republic

ARTICLE INFO

Editor: Marie Weiss

Keywords:

Analysis-ready data
Big data
Large-area mapping
Germany
Common agricultural policy
Time series
Land use intensity
Optical remote sensing
Multi-spectral data
PlanetScope

ABSTRACT

Spatially explicit knowledge on grassland extent and management is critical to understand and monitor the impact of grassland use intensity on ecosystem services and biodiversity. While regional studies allow detailed insights into land use and ecosystem service interactions, information on a national scale can aid biodiversity assessments. However, for most European countries this information is not yet widely available. We used an analysis-ready-data cube that contains dense time series of co-registered Sentinel-2 and Landsat 8 data, covering the extent of Germany. We propose an algorithm that detects mowing events in the time series based on residuals from an assumed undisturbed phenology, as an indicator of grassland use intensity. A self-adaptive ruleset enabled to account for regional variations in land surface phenology and non-stationary time series on a pixel-basis. We mapped mowing events for the years from 2017 to 2020 for permanent grassland areas in Germany. The results were validated on a pixel level in four of the main natural regions in Germany based on reported mowing events for a total of 92 (2018) and 78 (2019) grassland parcels. Results for 2020 were evaluated with combined time series of Landsat, Sentinel-2 and PlanetScope data. The mean absolute percentage error between detected and reported mowing events was on average 40% (2018), 36% (2019) and 35% (2020). Mowing events were on average detected 11 days (2018), 7 days (2019) and 6 days (2020) after the reported mowing. Performance measures varied between the different regions of Germany, and lower accuracies were found in areas that are revisited less frequently by Sentinel-2. Thus, we assessed the influence of data availability and found that the detection of mowing events was less influenced by data availability when at least 16 cloud-free observations were available in the grassland season. Still, the distribution of available observations throughout the season appeared to be critical. On a national scale our results revealed overall higher shares of less intensively mown grasslands and smaller shares of highly intensively managed grasslands. Hotspots of the latter were identified in the alpine foreland in Southern Germany as well as in the lowlands in the Northwest of Germany. While these patterns were stable throughout the years, the results revealed a tendency to lower management intensity in the extremely dry year 2018. Our results emphasize the ability of the approach to map the intensity of grassland management throughout large areas despite variations in data availability and environmental conditions.

1. Introduction

Grasslands are important ecosystems in the agricultural landscapes

of temperate zones both area-wise and considering the ecosystem services provided (Zhao et al., 2020). In Europe, permanent grasslands account for approximately one third of all agricultural areas (Huyghe

* Corresponding author at: Humboldt-Universität zu Berlin, Geography Department, Unter den Linden 6, 10099 Berlin, Germany.

E-mail address: marcel.schwieder@geo.hu-berlin.de (M. Schwieder).

<https://doi.org/10.1016/j.rse.2021.112795>

Received 10 April 2021; Received in revised form 29 October 2021; Accepted 3 November 2021

Available online 25 November 2021

0034-4257/© 2021 The Author(s). Published by Elsevier Inc. This is an open access article under the CC BY license (<http://creativecommons.org/licenses/by/4.0/>).

et al., 2014) and provide a broad range of ecosystem services, such as filter or retention functions, carbon storage as well as provisioning and recreational services (Gibson and Newman, 2019; Zhao et al., 2020). Grasslands offer habitats for endangered and key species and play a critical role for maintaining the biodiversity in agricultural landscapes (White et al., 2000; Zhao et al., 2020), which is, amongst others, critical for biological pest control, crop pollination and productivity (Tscharnkte et al., 2005). The economic value of grasslands is directly linked to the production of fodder for livestock farming, for which grasslands are either mown or used as pasture. Grasslands provide high-quality basic feed with low transportation and production costs when produced in the same area where livestock farming occurs. The productivity of grasslands is influenced by various factors, such as topography, soil condition, and climate. In this context, water supply is key, which is mediated through the soils' storage capacity and the ample and timely supply of water either through rainfall or shallow groundwater, demanding to adjust grassland management decisions to local environmental conditions. These management decisions, in turn, directly and indirectly impact ecosystem services provided by grasslands as well as their biodiversity (Allan et al., 2014; Le Clec'h et al., 2019; Wrage et al., 2011). A sufficient share of grasslands in the agricultural landscape as well as adapted management are therefore needed to maintain critical ecosystem functions.

High losses of permanent grasslands were observed in the last decades of the 20th and the first decade of the 21st century in several European countries, including France, the Netherlands and Germany. This development can be attributed to land conversions to arable land, urban areas and afforestation as well as to the abandonment of marginal range- and grasslands (Huyghe et al., 2014). Incentives such as the Greening program within the framework of the Common Agricultural Policy (CAP) were put into place in 2013 to halt this trend, aiming e.g., to foster the maintenance of permanent grasslands (EC, 2018). Monitoring of grassland areas is accordingly crucial to assess the success of such measures. Rough estimates of the extent of grasslands can be derived from national statistics and farmers' reports in the European Geospatial Aid Application (GSAA) system, based on which farmers can apply for subsidies within the CAP. However, information on the grassland productivity, which is influenced by the grassland management intensity (GLMI), is not well documented (Huyghe et al., 2014); (Smit et al., 2008). In addition to the use of such information for cross-compliance checks in the context of the CAP, knowledge of the intensity of grassland use is an important indicator for assessing the status and development of both faunal and floral biodiversity in agricultural landscapes (Klein et al., 2020). Although such data can be derived for individual parcels to monitor trends in grassland use intensity over several years (Vogt et al., 2019), such information is not available in a spatially explicit form on national scale.

In the last decades remote sensing has been shown to be a beneficial tool for large-scale monitoring of grasslands, e.g., management-related degradation processes in rangelands around the world (Bastin et al., 2014; Lewińska et al., 2020; Munyati and Makgale, 2009; Zhou et al., 2017). However, intensively managed meadows and pastures in Northern and Central Europe are managed differently than expansive rangelands and different climatic conditions do apply. This is due to the high diversity in spatial and temporal patterns of grassland extent and management intensity, which challenges commonly employed large-scale monitoring approaches that were developed for monitoring grazed rangelands. A common approach to map GLMI with remote sensing data is to estimate the number and timing of mowing events per season, which requires data of sufficient spectral, spatial and temporal resolution (Ali et al., 2016; Reinermann et al., 2020). Franke et al. (2012), for example, used multi-temporal RapidEye data, with a spatial resolution of 6.5 m in a study area in southern Germany and highlighted the use of high-resolution, multi-spectral and multi-temporal satellite data for monitoring GLMI. Their findings were confirmed by Gómez Giménez et al. (2017) who also used multi-temporal RapidEye data for

assessing GLMI in the Canton of Zurich in Switzerland. However, as high-resolution satellite data are commonly commercial, they are not freely available, which can result in high costs for regular area-wide mapping approaches. Kolecka et al. (2018) therefore made use of openly available Sentinel-2 data and highlighted the benefits of dense time series for mapping mowing frequency as an indicator of GLMI in the Canton Argau in Switzerland. In their study, the authors highlight the influence of data availability for an accurate mowing detection and stress the importance for an optimized cloud detection. Thus, several studies tested the use of Synthetic Aperture Radar (SAR) data that are not confined by cloud contamination. Tamm et al. (2016); Voormansik et al. (2016) and De Vroey et al. (2021) for example, emphasized the use of coherence time series derived from TerraSAR-X, RADARSAT-2 or Sentinel-1 in their respective case studies for mapping GLMI of European grasslands. Taravat et al. (2019) used Sentinel-1 time series and derived texture metrics in a multilayer perceptron neural network to detect mowing on a study site in Germany. Both optical and SAR based approaches assume that mowing events can be detected by sudden drops (optical) or increases (coherence) in dense time series of remote sensing data, see Voormansik et al. (2020). However, there are still uncertainties in the interpretation of SAR signals in the context of GLMI (De Vroey et al., 2021).

While these approaches have proven that it is possible to accurately map GLMI, most approaches had a regional focus to showcase the applicability of the respective method, while very few aimed to create information on a national or even larger scale. General change detection approaches that make use of Landsat data with a spatial resolution of 30 m × 30 m such as the Continuous Change Detection and Classification (CCDC; Zhu and Woodcock, 2014) or the Continuous monitoring of Land Disturbance (COLD; Zhu et al., 2020) algorithm, have shown to be able to detect major land cover changes over large scales. However, they were not designed for the detection of mowing events, as these are characterized by short-term mowing and regrowth cycles that frequently repeat during the course of one year in contrast to gradual or persistent land use changes. Stumpf et al. (2020) made use of Landsat time series with a spatial resolution of 30 m × 30 m to map grassland management for Switzerland. For Germany, Griffiths et al. (2020) derived a national dataset on GLMI for the year 2016 from the Harmonized-Landsat-Sentinel (HLS) dataset at 30 m spatial resolution (Claverie et al., 2018). They proposed a convex hull approach, which was used to model an undisturbed seasonal time series profile and identified deviations under the curve as mowing events. Even though the approach yielded comprehensible results, it was constrained by the limited data availability at that time and the 30 m spatial resolution, which enforced relying on interpolated time series that can suffer from omission of mowing events.

The few available broad-scale studies, however, are good examples of how to make use of the advances in satellite data availability, which tremendously increased with more freely available remote sensing data becoming available in open archives (Wulder et al., 2015), and which catalyzed the development of approaches that make use of dense time series in virtual constellations (Wulder et al., 2018). The use of such time series has become feasible across large areas since the advent of high-performance computing and advances in analytical capabilities and is supported by analysis-ready data (ARD) cubes that can be derived from highly automated processing workflows (Dwyer et al., 2018; Frantz, 2019; Gorelick et al., 2017; Lewis et al., 2017). These comprise optimized pre-processing, such as automated cloud and cloud-shadow masking (Frantz et al., 2018; Qiu et al., 2019; Skakun et al., 2019), spatial co-registration (Rufin et al., 2021) and the intercalibration of different sensor systems (Scheffler et al., 2020), which together enable to develop workflows and to integrate algorithms that allow large-scale analyses with a fine temporal and spatial resolution. In comparison to optical data, ARD data cubes that contain SAR data and cover large regions are still rare.

Accordingly, the overarching objective of this study was to develop a

reproducible mowing detection algorithm that uses dense optical Earth observation time series and allows mapping, describing, and understanding large-scale patterns of GLMI at high spatial resolution. Here, we explicitly build on the results of Griffiths et al. (2020) who were the first to produce a wall-to-wall map of GLMI at national scale. In addition, the algorithm shall prove its capability to produce robust results for years with different data availability and meteorological conditions. The study focuses on Germany where extreme droughts in the summertime in two out of the four years under investigation allow assessing the applicability of algorithms under highly diverse meteorological conditions. We employed combined Sentinel-2 and Landsat 8 time series covering the period of four years from 2017 to 2020 to investigate three specific research questions:

1. How accurately can the number and date of mowing events be detected for multiple years across Germany?
2. To what extent does the availability of clear-sky observations influence the quality of the mowing detection results?
3. How do droughts affect grassland management patterns?

2. Data and methods

2.1. Study area

With an area of about 357,000 km², the Federal Republic of Germany is located in Central Europe between the maritime West and the continental East, as well as between the warmer South and the cooler North. Germany is divided into five natural regions from North to South (Fig. 1): the (1) North and Baltic Sea coast and the North German Plain, (2) the Central Uplands, (3) the South German Scarplands and the Upper Rhine Plain, (4) the Alpine Foreland, and (5) the German Alps (Beierkuhnlein, 2017). Within these natural regions typical agricultural parcel sizes follow a North - South gradient, with higher shares of large parcels in the North and smaller parcel in the South (Destatis, 2019a). Germany has a humid temperate climate with warm summers and corresponds to a Cfb climate in the Köppen and Geiger classification (Beierkuhnlein, 2017). The long-term mean (1961–1990) temperature for Germany is 8.2 °C with an annual rainfall of approx. 788.9 mm (Imbery et al., 2021). The four years under consideration were characterized by varying meteorological conditions. 2018 to 2020 were the three warmest years on record since 1881 (DWD, 2018, 2019, 2020). The three years were not only characterized by generally warm temperatures but also by heatwaves and long periods of drought over the summer months, and a precipitation deficit that could not be compensated for over the following winter months (DWD, 2018, 2019, 2020). 2018 became known as the driest year since 1881, as there was too little precipitation from February to November (only 75%), while the years 2019 and 2020 almost reached average precipitation conditions (93% and 90%; DWD, 2018, 2019, 2020). In contrast to the following years, 2017 had a surplus in precipitation and cooler summer temperatures, especially in the north of Germany (DWD, 2017).

2.2. Grassland areas in Germany

Approximately 50% of the land area of Germany is used for agricultural production with 28% being permanent grasslands (Destatis, 2019b). We extracted the grassland areas from remote sensing-based crop type classifications for Germany for the years 2017–2019 with a spatial resolution of 10 m × 10 m, which was derived from time series of Landsat, Sentinel-1 and 2 and environmental data (maps online available; Blickensdörfer et al., 2021). Each of these annual classifications contain a grassland class with user's accuracies of above 90%. However, they include all types of grassland areas and do not differentiate between temporary and permanent grasslands in the individual years. For a fair comparison between the four years of our investigation period, we derived a consistent grassland mask that considers only pixels that have

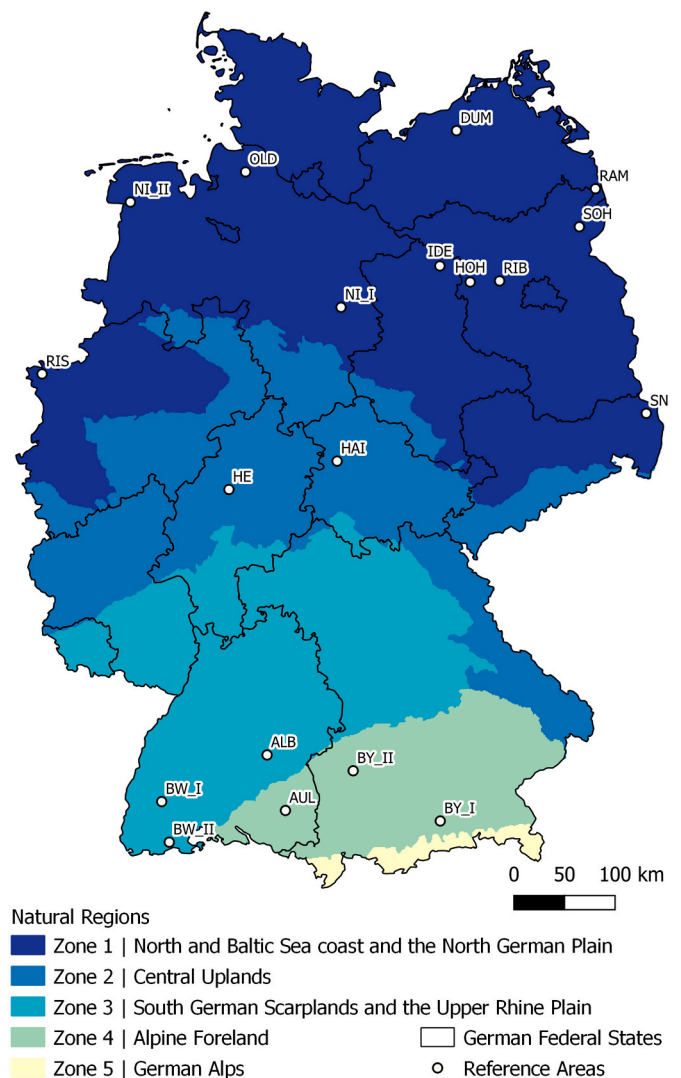


Fig. 1. Overview of the five natural regions of Germany and the distribution of the reference sites a) for which management information were available: Oldenburg (OLD), Ramin (RAM), Schorfheide (SOH), Ribbeck (RIB), Dummerstorf (DUM), Iden (IDE), Hohennauen (HOH), Riswick (RIS), Hainich (HAI), Schwäbische Alb (ALB), Aulendorf (AUL) and b) for which management information were derived from satellite time series: Lower Saxony I and II (NI_I; NI_II), Saxony (SN), Hesse (HE), Baden-Württemberg I and II (BW_I; BW_II) and Bavaria I and II (BY_I; BY_II).

been classified as grasslands in 2017, 2018 and 2019, which total to an area of around 40,000 km². Given its size and environmental gradients, as well the areal extent and variety of grasslands, the case of Germany allows for developing a transferable GLMI mapping approach for temperate grasslands.

2.3. Satellite and reference data

We used a harmonized time series derived from Sentinel-2 A/B Level 1C (Drusch et al., 2012) and Landsat 8 collection 2 Tier 1 L1TP data (USGS, 2021) including all available data from 2017 to 2020, with a cloud cover of up to 75%. All data were ingested in a data cube structure generated within the FORCE environment (v. 3.6; Frantz, 2019). All data were corrected for geometric and radiometric effects using the FORCE Level 2 Processing System. Radiometric correction included corrections for atmospheric, topographic, adjacency and BRDF effects (Buchner et al., 2020; Frantz et al., 2016a; Roy et al., 2017). Clouds were masked based on the Fmask algorithm (Frantz et al., 2018; Zhu et al., 2015; Zhu

Table 1
Number of reported/identified cuts in the reference data per year.

No. cuts	2018	2019	2020
0	–	–	4
1	18	25	16
2	29	18	56
3	20	12	71
4	31	30	28
5	10	21	4
6	–	–	1

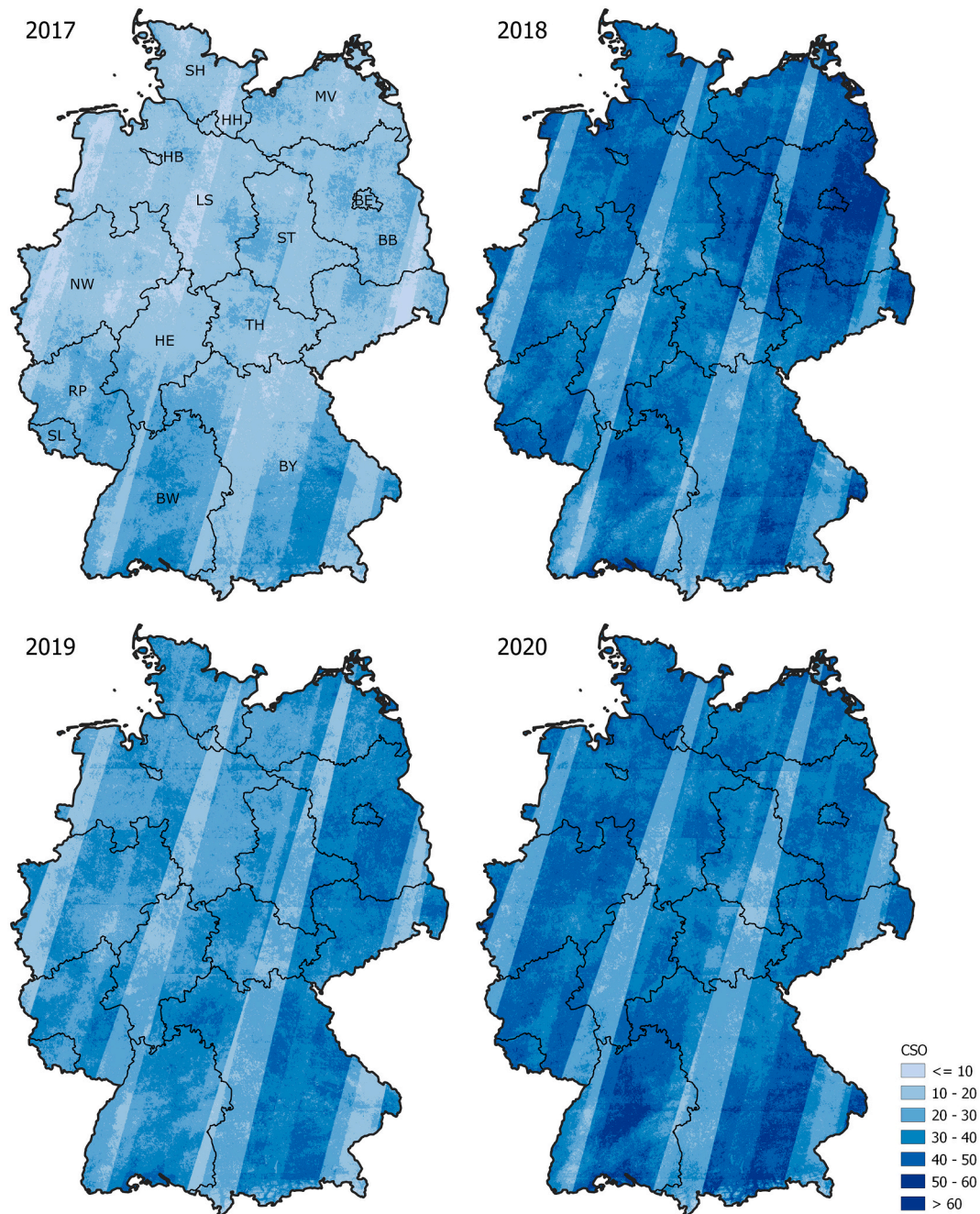


Fig. 2. Number of clear sky observations (CSO) in Germany from March to November for the years 2017–2020. Federal state boundaries with abbreviations of their names: BW: Baden-Württemberg, BY: Bavaria, BE: Berlin, BB: Brandenburg, HB: Bremen, HH: Hamburg, HE: Hesse, LS: Lower Saxony, MV: Mecklenburg-Vorpommern, NW: North Rhine-Westphalia, RP: Rhineland-Palatinate, SL: Saarland, SN: Saxony, ST: Saxony-Anhalt, SH: Schleswig-Holstein, TH: Thuringia.

and Woodcock, 2012). The Sentinel-2 scenes were co-registered to the Landsat 8 data to ensure the best possible geometric accuracy across different sensor systems for time series analyses (Rufin et al., 2021; Yan et al., 2018), reprojected to Lambert Equal Area projection (EPSG:3035) and stored as 30 km × 30 km tiles in a data cube structure (Frantz, 2019). Landsat 8 spatial resolution was adjusted to the 10 m Sentinel-2 spatial resolution by nearest neighbor resampling. For each pixel, the enhanced vegetation index (EVI) was calculated, as it can be related to vegetation biomass, reduces atmospheric influences and decouples the canopy signal from the background (Huete et al., 2002). In cases when Landsat 8 and Sentinel-2 acquired data at the same date, the mean value of both observations was used for creating the time series. Values above 1 and below 0 were set to “No Data”. This resulted in radiometrically and geometrically consistent cloud-free Sentinel-2 and Landsat 8 EVI time series that cover the entire extent of Germany.

Reference data on grassland management was available for 2018 and 2019 for the five main natural regions in Germany and include intensively and extensively managed grassland areas (Fig. 1). We thus covered the environmental gradient as well as large parts of the expected gradient in management intensity in Germany. The data were provided by partners from the Raminer Agrar GmbH & Co. KG, the Havellandhof Ribbeck GbR and the Agrargenossenschaft Hohennauen eG. Additional reference data were provided by partners from the agricultural research institutions of the chamber of agriculture Lower Saxony (Oldenburg) and North Rhine-Westphalia (Riswick), the state institute for agriculture and horticulture Saxony-Anhalt (Iden) and the center for agriculture Baden-Wuerttemberg (Aulendorf). Further reference data were available for the three biodiversity exploratories located in the regions Schorfheide, Hainich and Schwäbische Alb (Fischer et al., 2010). For 2018 a total of 92 reference parcels (~ 672 ha) and for 2019 a total of 81 reference parcels (~ 435 ha) were available, for which the number and dates of mowing events was reported (Table 1). We applied an inward buffer of 10 m, to assure that mixed pixels were excluded as well as to account for uncertainties in geo-registration between satellite and vector data (see S 1 for parcel details).

To evaluate the results for the year 2020 grassland parcels were manually digitized based on time series of PlanetScope data that cover the visible and near infrared spectral regions in four spectral bands with a spatial resolution of approximately 3 m (Planet Team, 2017). To ensure that the reference data are representative for a thorough validation, parcels were identified across Germany in selected regions that i) have high shares of grasslands (according to the grassland masked used) ii) cover a broad range of grassland management intensity (according to the mowing detection results) and iii) vary in the number of clear-sky-

observations (i.e., inside and outside orbit overlaps; Fig. 2). In total we used 257 PlanetScope images, covering the period March to November 2020 in eight selected regions (Fig. 1; see S2 for a list of acquisition dates per region). As some of these images did not cover the entire region or were influenced by cloud remnants, the high-resolution time series had partly long gaps and were thus complemented by Sentinel-2 and Landsat 8 data. From these dense time series mowing events were manually identified for a total of 180 grassland parcels using the EO Time Series Viewer (Jakimow et al., 2020).

2.4. Mowing detection

The above described EVI time series are non-stationary over time, as cloud cover and overlapping sensor orbits lead to substantial variation in data densities (Fig. 2). We thus developed a mowing detection algorithm that uses dynamic thresholds to account for these variations as well as for gradients in environmental conditions and varying management intensities. We identified mowing events as deviations from an assumed undisturbed phenology. The approach is pixel-based and includes the following: first, the season in which grassland growth and hence relevant mowing events can be expected (here: 1st of March to 15th of November) is defined. The pre-processed EVI time series is used to identify up to five local maxima within the user defined grassland season. The mid-season peak is identified as the absolute maximum EVI value in a period in which maximum grassland growth is expected (here between: 30th of April and 28th of August), subsequently further peaks can be identified before and after this peak with a temporal distance of at least 15 days if data availability allows. These peaks are used as vertices and EVI values are linearly interpolated between the vertices for each date when an observation was available in the time series, hence forming an upper envelope that approximates an ideal, non-disturbed growing season (Fig. 3).

The residual between the interpolated and the original EVI values is calculated, as well as the difference between the values of two consecutive observations ΔY . Then, five rules are applied that qualify the detected differences as potential mowing events:

1. The residual must exceed a threshold, which is defined for each pixel as the mean value of all absolute residuals within the grassland season. To avoid misclassifications for pixels with values slightly below or above the threshold, we accounted for variations around this threshold (compare Frantz et al., 2016b). For that, we drew 100 random values from a Gaussian normal distribution around the derived threshold with a standard deviation of 0.02 and tested them

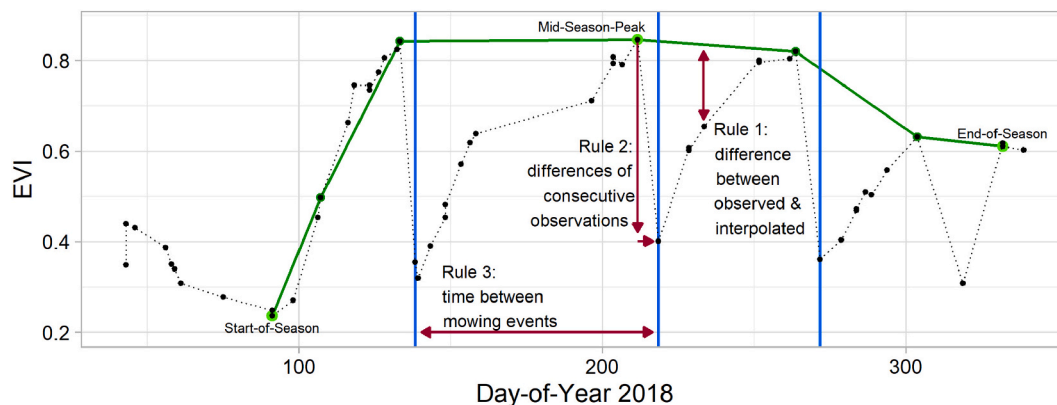


Fig. 3. Example of a grassland phenology as captured by an integrated Landsat 8 and Sentinel-2 EVI time series, with three detected mowing events. The green dots mark the defined start and end of season, the mid-season peak, and the additional local EVI maxima. The green line depicts the linear interpolation. The blue vertical lines mark mowing events as identified by the algorithm. If rules one to three are positively evaluated, rule four checks whether grassland regrowth can be identified between two mowing events. Mowing events that are followed by an unnaturally quick regrowth are excluded by rule five. (For interpretation of the references to colour in this figure legend, the reader is referred to the web version of this article.)

against the calculated difference. The potential mowing event qualifies for the next rule, if at least 40 of those tests were positive.

2. ΔY between two consecutive observations must be larger than an adaptive threshold. This rule depicts the main characteristic of a mowing event – a sudden drop in EVI between two observations. The threshold is defined per pixel as the standard deviation of the original EVI time series for the defined grassland season, to account for the regional variations in land surface phenology.
3. Potential mowing events must be more than 15 days apart from each other, as this depicts real-world regrowth potential and management opportunities.
4. Between two potential mowing events, there must at least be one observation with a value higher than the preceding one (i.e., a positive ΔY), as there must be regrowth to justify another mowing event.
5. Mowing events followed by unnaturally quick regrowth, i.e., ΔY larger than a user defined fixed threshold (here: 0.15) within 5 days, are excluded. This pattern is likely caused by an undetected cloud or cloud shadow.

The results are written into a raster, which includes the number of detected mowing events, along with the date for each event (Fig. 4). Additionally, the output contains pixel-wise information on the number of clear sky observations for the defined grassland season.

2.5. Accuracy assessment and influence of data availability

We validated the results for the years 2018, 2019 and 2020 with the available reference parcels. For each pixel within a parcel of the reference data, the predicted number and dates of mowing events was compared to the ones reported by the data providers. From this comparison we calculated the mean absolute percentage error (MAPE) of the number of mowing events. The MAPE prevents values from cancelling each other out and relates the error to the number of reported events in the reference data. If zero mowing events were reported for one parcel, the calculation of the MAPE was corrupted by dividing by zero. In case we predicted zero mowing events and had zero reference mowing events we set the MAPE to 0. In case we falsely predicted mowing, we set the MAPE to 100%. It has to be noted that the MAPE can, due to its definition, exceed 100% in cases where we predict more mowing events than reported in the reference. Subsequently the absolute difference between the dates of the detected mowing events and the nearest reported mowing date (offset) was calculated and averaged per pixel.

The MAPE is based on the number of mowing events only and does not account for the temporal domain. Therefore, we additionally calculated precision, recall and f-score of the mowing detection based on true/false positives and false negatives, as these measures qualify to assess the accuracy of imbalanced classification results (De Vroey et al., 2021; Sokolova et al., 2006). Precision can also be referred to as user's accuracy and recall as producer's accuracy, while the f-score is a combination of both. Using the f-score avoids an over-optimistic validation, as it does not consider true negatives, which are frequent in rare event detection approaches. Therefore, we considered the algorithm as binary classification of a time series, classifying each observation either as mowing event or no mowing event. A predicted mowing event qualified as true positive if it was predicted within a time window of three days before and no later than 12 days after a reported reference mowing event. This time window approach enables to account for discrepancies e.g., due to the temporal resolution of the satellite data or reported mowing events that took longer than one day on one parcel. Using this procedure, we obtained a confusion matrix for each pixel within a reference area, which we finally summed either per region or on a national level to derive accuracy measures for comparisons on various scales.

We analyzed the influence of data availability on the results with two approaches. First, we performed a linear regression with the number of available clear-sky observations (CSO) as predictor and the f-score as

response variable. As this analysis was restricted to the years in which reference data were available, we randomly sampled 500,000 pixels within the final map to analyze the relationship of CSO and the predicted number of mowing events and to assess if more observations in general lead to a higher detection rate of mowing events. Therefore, we used a generalized linear model (GLM) with CSO as predictor and the number of mowing events as response variable. More specifically, a B-spline with three knots was used to enable the model to depict changing relationships between the variables. For the modelling, the CSO variable was log transformed and rescaled.

The amount of detected mowing events was compared between the years on the level of the 13 federal states of Germany (the city states Berlin, Bremen and Hamburg were excluded from the comparison).

3. Results

3.1. Detection of mowing events

Annual maps of GLMI were derived for the years 2017–2020 covering the entire extent of Germany (Fig. 9). The comparison with the reference data showed that we detected fewer mowing events than reported in 2018 and 2019 (Table 2 and S 3). The MAPE in the number of detected mowing events was 40% (2018), 36% (2019) and 35% (2020; Table 3). The detected mowing events had an average absolute offset of 11.25 (2018) and 7.47 (2019) days regarding the dates of the detected mowing events. The f-scores differed amongst the regions, with highest values in Riswick (RIS), Randow Bruch (RAM) in 2018 and Schwäbische Alb (ALB;) and Aulendorf (AUL) in 2019. Lowest values in both years were in the lower Havel alluvial plain (HOH; Table 2).

The f-score is in 2018 despite Hohennauen in all study regions above 0.5 and up to 0.75 in Riswick. In 2019 f-scores were in Schorfheide and Hohennauen below 0.5 and values range up to 0.85 in Schwäbische Alb. The aggregated assessment shows comparable f-scores for the natural regions Zone 2 to 4, while the median f-score is lower in Zone 1 (Fig. 5). This pattern is influenced by the study site Hohennauen (Table 2 and Fig. 1) which is located in a region without orbit overlap (Fig. 2) and was in both years evaluated with the lowest f-score. The f-score in 2020 was derived from image-based reference data and identified mowing dates are thus dependent on the availability of clear-sky-observations and consequently do not exactly align with the reported reference data. Nevertheless, the overall f-score of 0.67 is comparable to the f-score of 2019 (0.64). Also, the overall MAPE is in the same range as in the previous years (35–40%). The study area in Saxony performed the worst in terms of MAPE with a value of 85%, but still has a high f-score of 0.76. For the f-scores, no region stands out as they are all close to the overall average of 0.67 (range between 0.61 and 0.78) and no clear distinction can be identified between regions with or without orbit overlaps in 2020.

In contrast to the f-score, the MAPE evaluates all detected mowing events and neglects temporal differences. Despite Hohennauen all MAPE values are below 0.5 in 2018. In 2019 Hohennauen and Schorfheide are evaluated with a MAPE of above 0.5. The average absolute offset is in 2018 below 15 days for all study sites. In 2019 only Hohennauen has an offset of more than 15 days.

3.2. Impact of data availability

The different accuracy measures showed that a higher data availability was not necessarily associated with higher f-score values (see Table 2). Hainich and Schwäbische Alb for instance achieved a higher f-score in 2019 despite a lower data availability. The scatter plots between CSO and f-score per parcel show a rather dispersed distribution, even though the fitted linear regression indicates a positive relation (Fig. 6). Higher f-score values can be observed in both years with an increasing amount of CSO. In 2020 there is no visible relationship between CSO and the f-score (S 4).

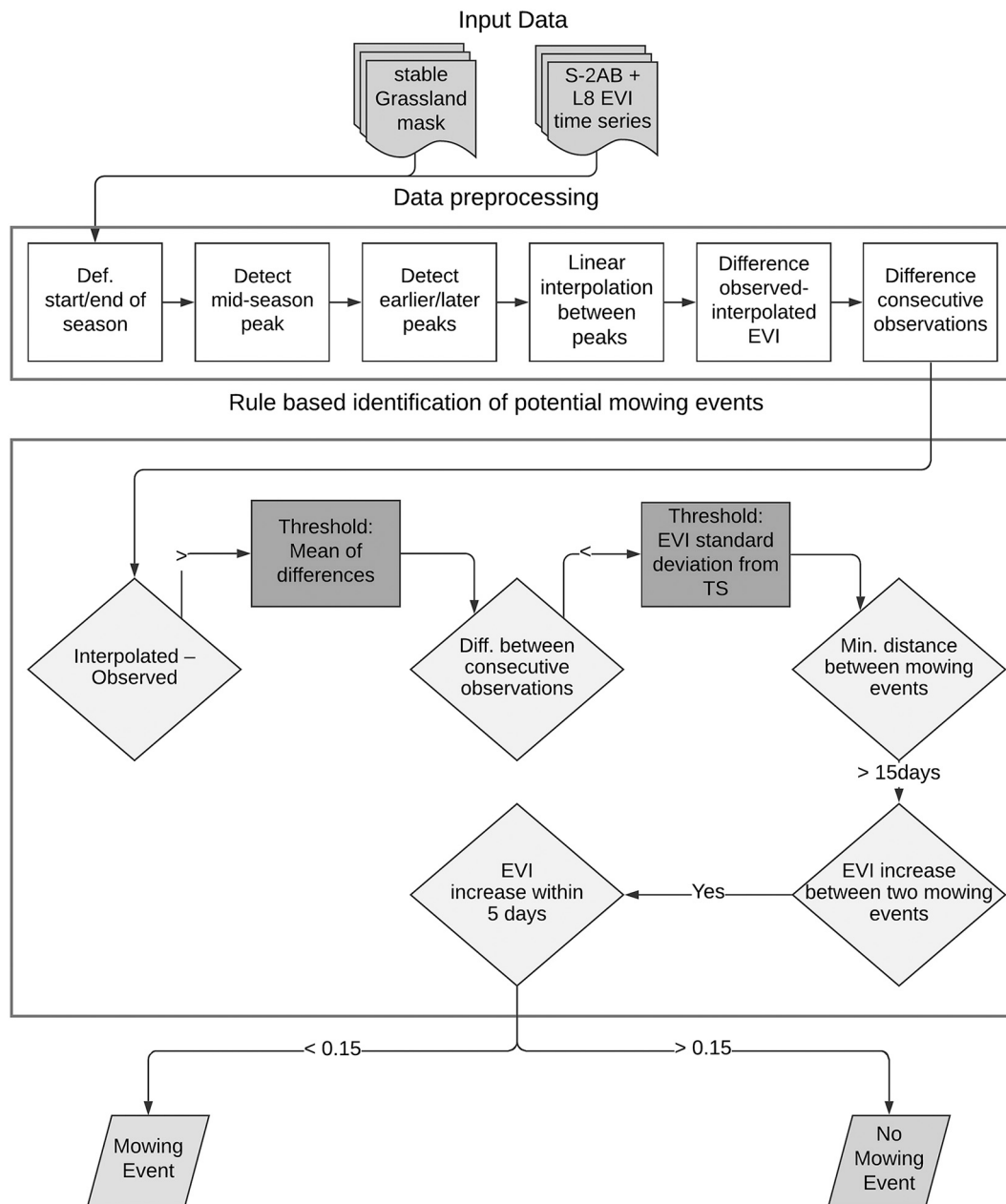


Fig. 4. Structure of the mowing detection algorithm. From top to bottom: (1) Input data, (2) data processing, (3) rule-based identification, and (4) output.

The analysis based on 500,000 random samples revealed that the number of CSO was substantially lower in 2017 as compared to the following years, as 2017 was earlier in the Sentinel-2 constellation lifetime and cloudiness was substantially higher that year (Fig. 7). While in 2017 less observations were related to fewer mowing events, this cannot be observed for the later years.

This assessment was quantitatively confirmed by the GLM between the number of CSO and detected mowing events, which showed a significant relation ($p < 5\%$) for all years. Even though the effect size of CSO on the number of mowing events was small for all years except for 2017, there is a threshold where the effect of the number of CSO changes (Fig. 8). This threshold occurred at about 16 observations with small variations between the four years. Thus 16 observations were the threshold, where more observations not necessarily resulted in more detected mowing events. Below that point, there is a strong positive relationship in all years. The distribution density plot of CSO shows that the years 2018 and 2020 had a very similar, bimodal distribution. The

years 2019 and 2017 were unimodal distributed with peaks around CSO of 16 (2017) and 28 (2019). This distribution indicates that the results for 2017 are likely to be more influenced by data availability than the other years.

3.3. Spatial and temporal patterns of mowing events

The broad-scale patterns revealed areas with consistently different levels of GLMI in all four years (Fig. 9). The resulting maps show rather homogeneous parcels and depict the structural differences in the agricultural landscape across Germany with comparably large parcel sizes in the Northeast and East (Fig. 9; C) and smaller parcel sizes in the Northwest (Fig. 9; A and B), West (Fig. 9; D) and South (Fig. 9; E and F). Highly intensive grassland use can be observed in the alpine forelands in southern Germany and in the lowlands of northwest Germany. This pattern of management intensity is consistent throughout all years.

We detected one to three mowing events on the vast majority of

Table 2
Validation results for the mowing event detection for the years 2018 and 2019.

Region (no. of reference parcels and area in ha, for 2018/2019 respectively)	F-score	MAPE [%]	Offset [days]	Data availability (median)	F-score	MAPE [%]	Offset [days]	Data availability (median)
	2018				2019			
Oldenburg (OLD) (6/5; 39/36)	0.61	40	8.90	38	0.77	34	4.18	26
Ramin (RAM) (7/0; 101/0)	0.70	9	8.40	48	–	–	–	–
Schorfheide (SOH) (14/12; 33/34)	0.62	24	14.16	49.5	0.49	60	9.66	36
Ribbeck (RIB) (6/0; 139/0)	0.58	40	13.92	44	–	–	–	–
Iden (IDE) (1/0; 13/–)	0.68	96	1.04	42	–	–	–	–
Hohennauen (HOH) (10/10; 128/128)	0.21	57	14.08	28.5	0.43	52	19.51	18.5
Riswick (RIS) (3/3; 43/43)	0.75	49	4.93	38	0.58	43	6.76	30
Hainich (HAI) (10/11; 39/45)	0.51	23	9.63	35.5	0.66	16	3.9	32
Schwäbische Alb (ALB)(14/12; 77/72)	0.56	30	11.72	32	0.85	12	5.08	29
Aulendorf (AUL) (16/16; 38/38)	0.55	36	9.91	35	0.82	30	4.84	30
Dummerstorf (DUM) (0/2; 0/15)	–	–	–	–	0.61	43	6.84	31.5
Overall	0.58	40	11.25	–	0.64	36	7.47	–

Table 3
Validation results for the mowing event detection for the year 2020 based on mowing events identified from combined time series of PlanetScope, Sentinel-2 and Landsat 8 time series. Ovl or non-ovl indicates if the study site is located in an orbit overlap or not.

Region (no. of reference parcels and area in ha)	F-score	MAPE [%]	Offset [days]	Data availability (median)
BW_I; non-ovl (31; 55)	0.61	33	9.54	19
BW_II; ovl (21; 18)	0.62	31	7.72	45
BY_I; ovl (32; 32)	0.71	28	4.67	48
BY_II; non-ovl (20; 31)	0.64	35	5.04	23
HE; non-ovl (30; 55)	0.69	35	6.39	23
NI_I; ovl (20; 26)	0.63	47	4.77	43
NI_II; ovl (20; 26)	0.78	29	3.86	32
SN; ovl (6; 20)	0.76	85	8.61	40
Overall	0.67	35	6.2	–

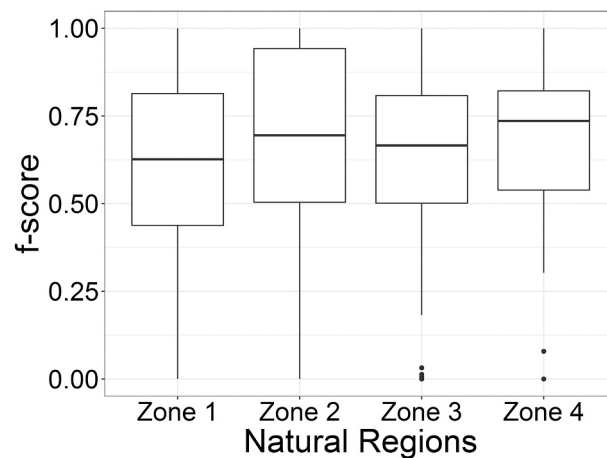


Fig. 5. Combined boxplots of all f-scores per natural region in Germany for years 2018, 2019 and 2020.

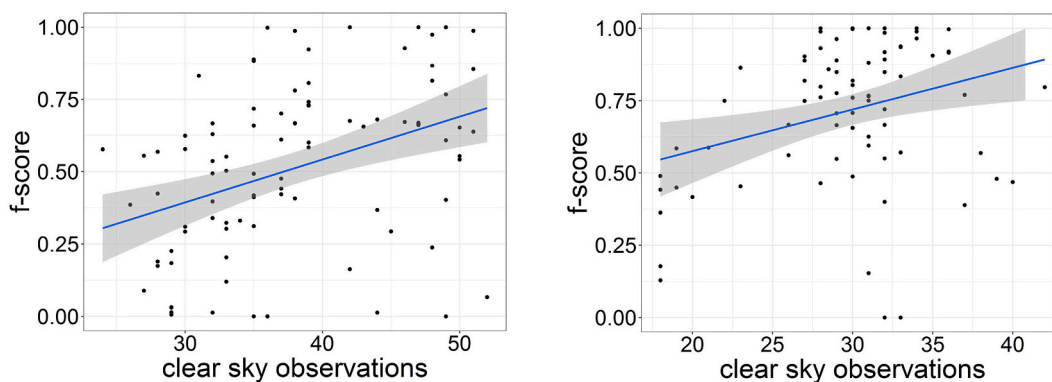


Fig. 6. Scatterplots of average CSO per parcel on the x-axis and average f-score per parcel on the y-axis for the years 2018 (A) and 2019 (B); Note the different x-axis ranges.

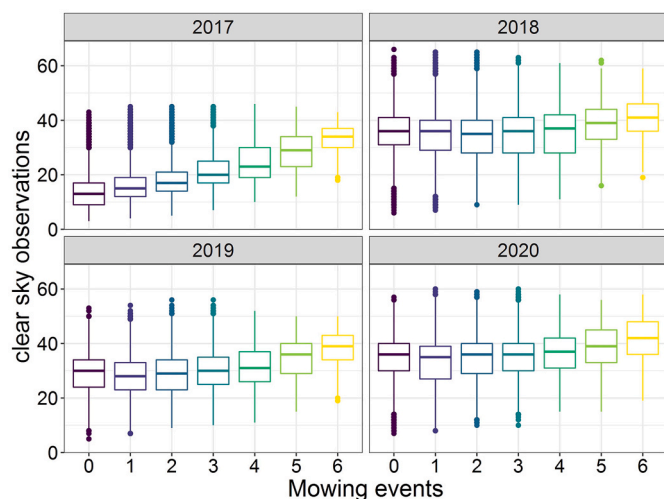


Fig. 7. Distribution of the number of clear-sky observations per number of detected mowing events for each year based on 500.000 random samples.

grassland areas for all four years. In 2017, 2019, and 2020, we detected two mowing events on between a quarter to a third of the overall grassland area of Germany, followed by one mowing event detection. The extreme drought year of 2018 was the only year for which most grasslands were mown only once. It is also 2018 in which grasslands stay unmown twice as often as in the other years (Fig. 10).

The distribution of detected mowing events differed between the individual federal states (Fig. 9 Fig. 11), with higher shares of intensively mown grasslands in Southern Germany. While the general distribution of detected mowing events was comparable between the years 2017, 2019, and 2020, we detected differences between 2018 and the other years in seven out of the analyzed 13 federal states (S 5). A shift to less intensively used grasslands in 2018 was observed, indicated by higher shares of zero and one mowing events. This trend is less pronounced in the southern states of Bavaria and Baden-Wuerttemberg, in comparison to northern states i.e., Brandenburg, Schleswig-Holstein and Lower Saxony, where the share of unmown grasslands more than doubled in 2018 in comparison to 2019 (Fig. 11). In Baden-Wuerttemberg, Brandenburg, and Schleswig-Holstein the share of grassland areas with one detected mowing event increased by around 10% in 2018.

3.4. Dates of mowing events

The timing of the detected mowing events differed between the individual federal states, and it was observable in all years that the median

dates of the detected events do not overlap (Fig. 12 and S 6). In comparison to the other years, the variations around the median date were highest in 2017, which was especially pronounced in the timing of the first and second mowing event. The first mowing event in 2018 was detected earlier than in 2019 in all federal states but not necessarily earlier than in 2020. Largest differences in median dates between 2018 and 2019 are in Saxony (19 days), Baden-Wuerttemberg (17 days) and Bavaria (15 days). Lowest interquartile ranges were also detected in 2018 in Saxony-Anhalt and Lower Saxony. The results revealed that the timing of the second and third detected mowing event varied stronger around the median, with the median itself also not occurring at the same time of the year across the federal states. Interestingly, in most of the federal states the results showed that the fourth and, in some cases, the fifth mowing event was detected earlier from 2018 onwards.

4. Discussion

Spatially explicit knowledge on grassland extent and management is critical to understand and assess the impacts of land-use intensity on ecosystem services and biodiversity. Even though remote sensing-based approaches have been shown valuable to gather such information, large-scale mapping approaches are still scarce (Reinermann et al., 2020). To bridge this gap, we made use of an ARD cube that contains co-registered Sentinel-2 and Landsat 8 collection 2 data, in combination with an advanced mowing detection algorithm that uses adaptive per-pixel thresholds. In contrast to approaches with fixed thresholds (e.g., Kolecka et al., 2018; Griffiths et al., 2020), the proposed use of adaptive thresholds facilitates to account for variations in land surface phenology and data availability. This enabled us to map mowing events for the years 2017–2020 for the considered grassland areas in Germany, to assess the results with a representative reference data set and to investigate the influence of data availability on the amount of detected mowing events.

4.1. Mowing detection accuracy

Validation of our results with reference data available in two years and a third year of manually digitized reference data confirmed the applicability of the proposed approach. On average, the f-score was at about 0.6 for all years while only one test site exhibited values below 0.5 in 2018 and 2019 (Hohennauen). These values strongly influence the pixel-based overall measures, as Hohennauen was the second largest reference site covering a total of 128 ha in a region without orbit-overlap and thus fewer clear-sky observations with an equal distribution throughout the season. Here, in 2018 and 2019, the precision is higher than the recall value, suggesting that the algorithm detects less false positives than false negatives (S 3). The trend of precision being higher than recall can also be observed in the global values (for 2018: 0.68 vs

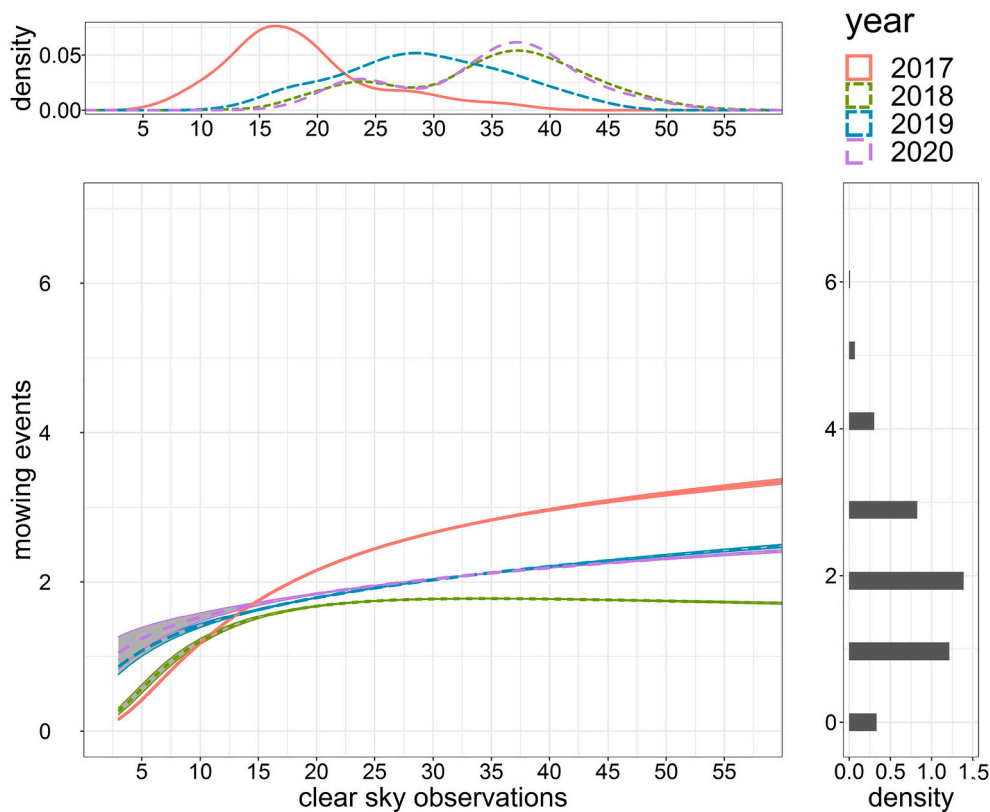


Fig. 8. Plot of CSO number against the number of mowing events for the years 2017–2020. The histograms show the CSO data distribution for the four years (top) and the detected mowing events (right side). The graphs show the yearly fitted splines.

0.50), suggesting that the results are conservative as the approach tends to detect fewer rather than too many mowing events, which should be considered in subsequent analyses. In contrast to the f-score the MAPE refers to the absolute number of mowing events predicted vs reference and does not consider the correct timing of the predicted mowing. The overall MAPE values are consistently low for all years. However, in the Saxony study area we obtained a high f-score despite high MAPE. This is likely because the MAPE is more sensitive to overestimation than underestimation. In these cases, the MAPE can exceed 100%, which is what happened in Saxony in two parcels and thus biased the overall value.

Next to the availability and distribution of CSO, mowing events may remain undetected when only a small amount of biomass was extracted. This might, for example, be the case when a clean-cut is applied to meadows or pastures, which is rather intended for maintenance of the grasslands than for biomass extraction. This results in subtle signal changes in the time series for which the adaptive thresholds might not be sensitive enough. These cases were also hard to identify in the high-resolution time series. However, more sensitive adjustment of the thresholds e.g., by enlarging the Gaussian distribution or the number of positive evaluations, could lead to overestimations in other regions, a dilemma also reported by [De Vroey et al. \(2021\)](#), who estimated mowing events from coherence time series. Identifying a threshold of extracted biomass that needs to be crossed could help to overcome this limitation, but this would require sufficient reference data on the amount of extracted biomass. Although not all mowing events reported in the reference data were detected, the results show that the algorithm can cope with the non-stationary data availability and enabled for the first time the monitoring of grassland management over large areas with strong environmental gradients in several years. This is confirmed by the f-score, which is quite stable across natural areas and years, whereas Zone 1 in the North of Germany shows the lowest median f-score values ([Fig. 5](#)). This might partly be caused by Hohennauen (Zone 1), which is not in an overlap region, suggesting that systematic differences in data

availability have a bigger impact on the f-score than the environmental gradient within Germany.

4.2. Influence of data availability

For 2018 and 2019 the relationship of CSO and the f-score per parcel suggests that increasing CSO will incrementally increase mowing event detection accuracy. A higher number of CSO increases the probability to include data from critical points in time, i.e., before and after a mowing event. In 2020 no relationship between CSO and f-score can be observed, which might be due to the difference in how the reference data were generated. In 2020 the reference data were manually generated and partly relied on the same data as the mowing detection algorithm. In this case the reference data are not fully independent and resulting relationships may differ, as we cannot compare our results to true mowing events and dates. Our results thus suggest that the distribution of CSO is more important than the sheer number of CSO, indicated by high f-scores related to an average number of CSO. However, it must be kept in mind that the f-score includes the temporal domain, as detected events are only counted as true positives, when they are within a temporal window of 3 days before or 12 days after the reported mowing event. Detected mowing events outside this temporal window are not considered, which can subsequently lead to low f-score values.

A positive relationship between CSO and the numbers of predicted mowing events was only found up to a certain number of CSO ([Fig. 8](#)). This is especially pronounced in the 2017 results, when cloud cover was overall high, and Sentinel-2 B was only available since the second half of the year ([Barsi et al., 2018](#)), but negligible in the following years when more data were available and fewer cloud contaminations hampered data acquisitions. We found that this relationship holds up until a minimum number of 16 observations is available, which still is not always met with our current observing capabilities in regions that are not within orbit overlaps ([Fig. 2](#)). These data gaps are visible in the GLMI

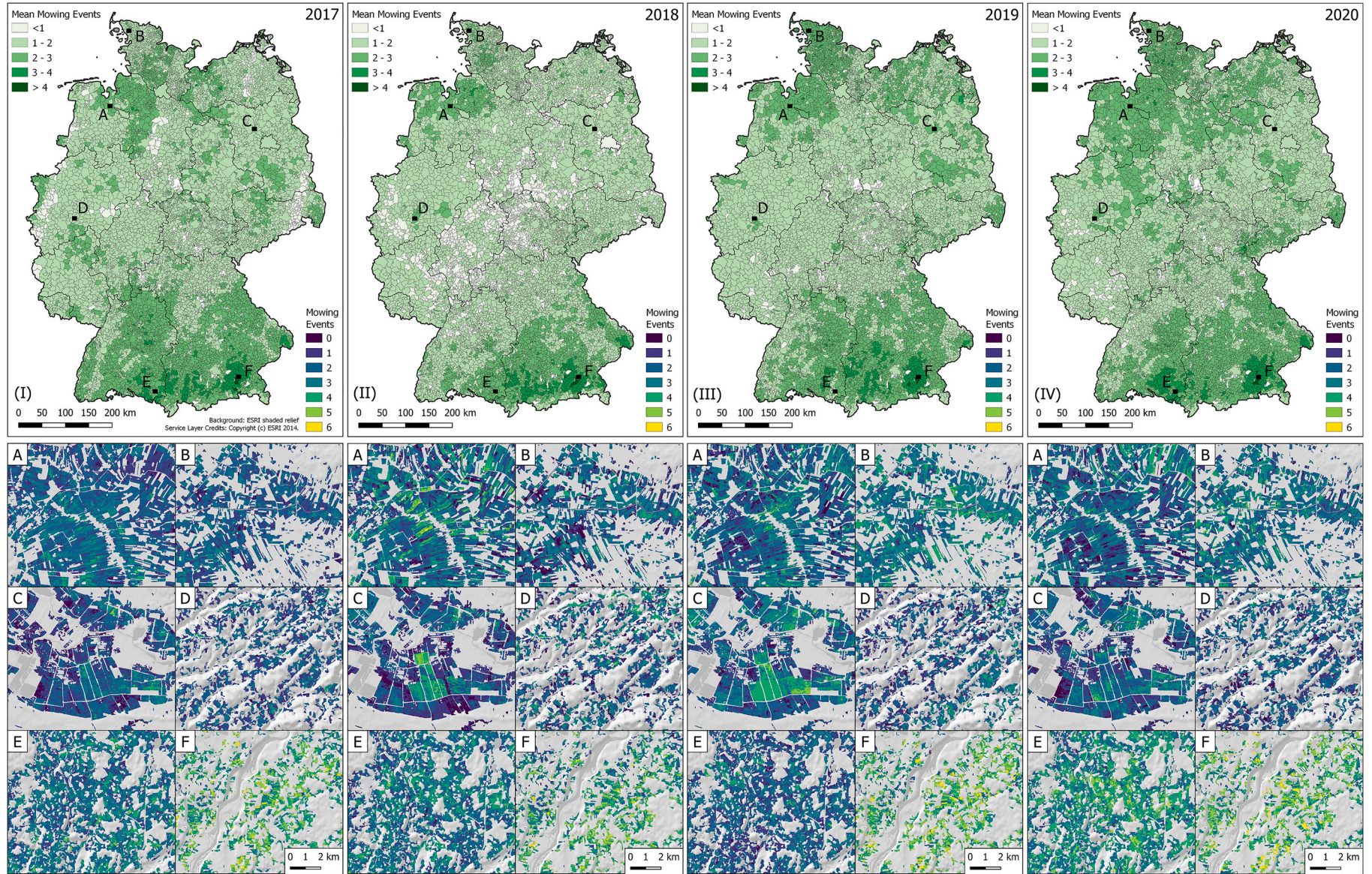


Fig. 9. Maps of the average number of mowing events in Germany on municipality level for the years 2017 (I), 2018 (II), 2019 (III), and 2020 (IV). Insets show selected regions with varying GLMI in the federal states with the highest shares of grassland (see Fig. 10): Lower Saxony (A), Schleswig-Holstein (B), Brandenburg (C), North Rhine-Westphalia (D), Baden-Württemberg (E), and Bavaria (F). The maps can be explored in an interactive webviewer: <https://ows.geo.hu-berlin.de/webviewer/mowing-detection/>.

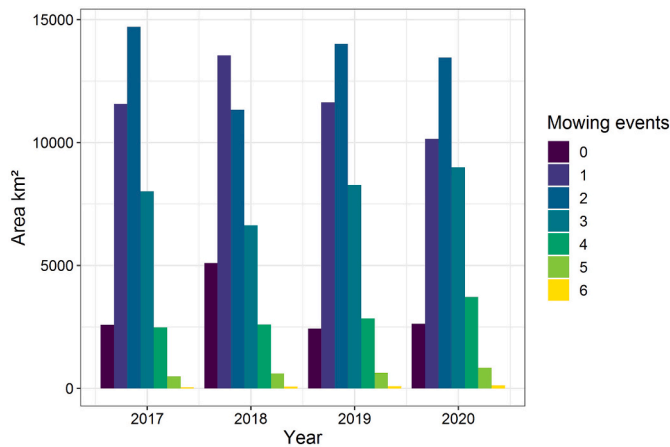


Fig. 10. GLMI as defined by the area of grassland relating to the number of mowing events for the years 2017–2020. The areas shown are derived from the pixel count and are not corrected for potential errors.

map for the year 2017 as they led to a systematic underestimation of mowing events, when the general data availability was not as high as in the following years (compare Fig. 2). This becomes increasingly problematic towards the South and may thus hamper comparable analyses in the context of CAP in other European countries. The launch of Landsat 9 and the planned launches of Sentinel-2C, and –2D in 2021/24/25 would enable to increase the density of optical time series — but only if all sensors remain active. This operation scheme is, however, not envisaged as Sentinel-2A will be taken offline once Sentinel-2C becomes operational. Another option could be the integration of data from other

sensors e.g., that are mounted on low-orbit satellites with a potential revisit time of up to one day (Houborg and McCabe, 2016). Promising cubesat data fusion approaches have recently been presented (Houborg and McCabe, 2018) and benefits of fusing Sentinel-2 with PlanetScope time series have been shown e.g., for daily LAI estimations (Sadeh et al., 2021). However, considerable calibration efforts would need to be taken. The Landsat-Sentinel-2 virtual constellation was planned for consistency (Drusch et al., 2012) and is being rigorously cross-calibrated (Helder et al., 2018), thus any addition to this virtual constellation shall meet these calibration requirements.

Another option to overcome data gaps in cloud-prone periods of the year or areas with systematic data gaps could be the integration of SAR data into the analysis. While the usefulness of SAR data for detecting grassland management has already been tested in several studies with a regional focus (De Vroey et al., 2021; Tamm et al., 2016, Lobert et al. accepted), mowing detection algorithms that make use of SAR and optical data together are still scarce. Even though mowing events can be identified in SAR time series, additional factors such as topography, parcel size and shape influence the results and there are still signal interactions that need to be further explored (De Vroey et al., 2021). Another challenging factor in the analysis of SAR data is the speckle effect on grasslands. This hampers pixel-wise analyses on a spatial resolution of 10 m × 10 m and makes object-based analyses mandatory for which (Wesemeyer et al., 2021) proposed a promising approach that enables to identify areas of homogeneous grassland management based on Sentinel-1 and Sentinel-2 time series. Once time series are corrected for these issues, they may complement the proposed approach, as shown for a test site in Brandenburg (Schwieder et al., 2019).

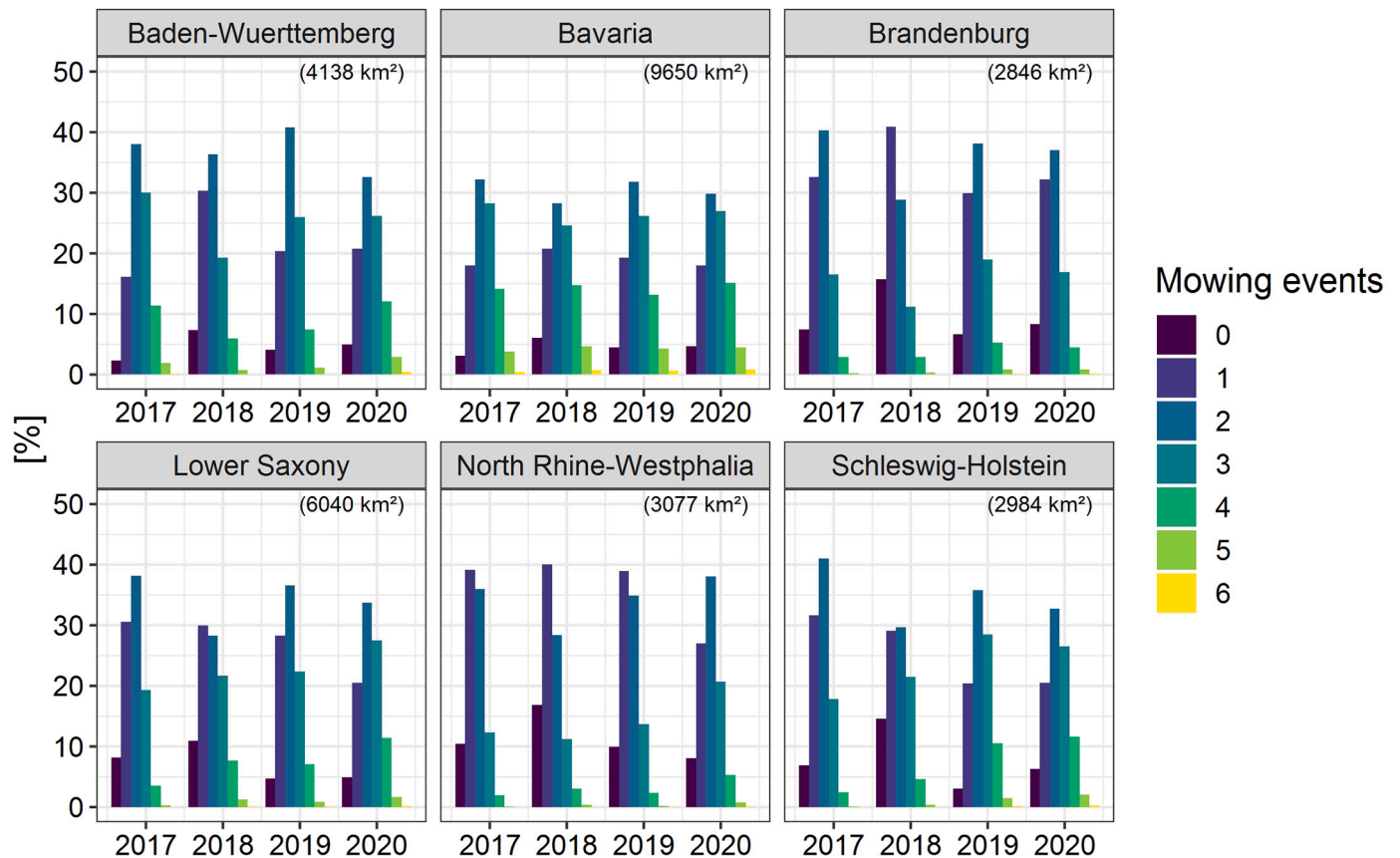


Fig. 11. Detected mowing events for those federal states of Germany with a share of more than 2500 km² of grasslands (number in brackets). See S 2 for the other federal states.

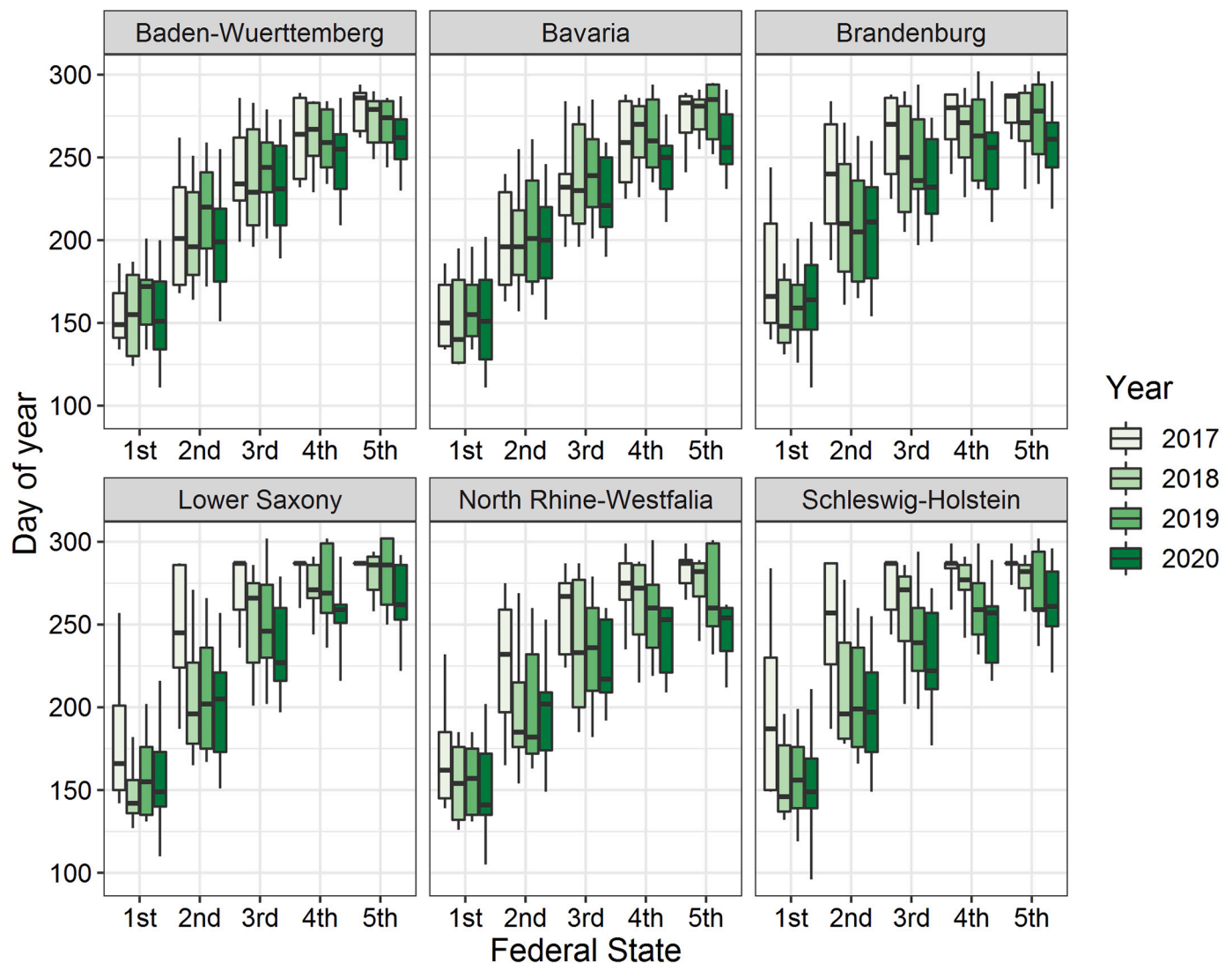


Fig. 12. Day of year of mowing events for all years in six federal states. The whiskers end at ± 1.5 times the interquartile range.

4.3. Patterns of grassland-use intensity in Germany

Spatial information in maps and in the derived statistics revealed similar general patterns of grassland-use intensity on a national as well as on the federal state level throughout all four years, indicating the transferability of the proposed approach in space and time. Comparing our results to Griffiths et al. (2020) reveals that we map an overall comparable pattern in terms of spatial distribution of grassland-use intensity and timing of mowing events as compared to 2016. However, between 2017 and 2020, we detect a considerably lower share of grassland areas without mowing activity, which was estimated to be above 25% in 2016 (Griffiths et al., 2020). While Griffiths et al. (2020) provided a first attempt to map temperate grassland use intensity on a national scale from dense HLS time series, their results were hampered by limited Sentinel-2 data availability at that time, as well as the 30 m spatial resolution of the time series. Thus, it was necessary to overcome data gaps by using best-pixel-composites and a linear interpolation to create equally spaced time series as input for their analyses. However, temporal resampling and gap filling approaches are problematic for the identification of subtle changes in time series and might have led to the overestimation of areas without mowing events in 2016. Our results highlight that data densities created from fully operational Sentinel-2 and Landsat 8 image acquisition from 2017 onwards is as much a

prerequisite as the biomass regrowth-related thresholding for frequent mowing event detection. The underlying algorithm is based on general knowledge about mowing process, which is mainly associated with a sudden removal of biomass. Even though machine learning approaches have been shown to accurately identify mowing events (e.g., Lobert et al., 2021), such a process-based approach enables to detect mowing events, to understand how certain output is produced and thus allow for adjustments if the algorithm is used e.g., in different management regimes.

However, our study lacks a separation of meadows and pastures, which can be a major confounding factor for remote sensing-based detection of mowing events (De Vroey et al., 2021). Nevertheless, we assume that due to the adaptive thresholds of the proposed approach, the management intensity of pastures is also reflected to a certain extent. On the one hand pastures are commonly mown once or twice during the seasons to clean the turf, which should be recognized in the time series signal. On the other hand, pastures in Germany are often managed with a rotational grazing scheme, in which herds stay on small paddocks for a few days only, before they are moved to a neighboring paddock (Mielke and Wohlers, 2019). Depending on the size of the herd as well as on the size of the parcel, the biomass removal is comparable to a mowing event. Thus, grazing with a large stock density may lead to a signal very similar to a mowing event (De Vroey et al., 2021). Extensive grazing on the

other hand with a lower stocking density leads to a slower biomass removal, which would probably not be detected by our algorithm as a “mowing event”. Also, grazing with a lower stocking density might lead to a more heterogeneous signal in space, as some livestock graze the plants in order of their preference, which could be the reason for the salt and pepper effect in the GLMI maps that we sometimes observed. Separating grassland uses prior to analysis might help to overcome this limitation but is still an unsolved challenge. Combining our additional outputs, such as the descriptive EVI time series statistics together with spatially explicit reference data could enable to identify phenological variations that allow to separate pastures from meadows, which should be tested in follow-up studies.

Our results suggest that the low precipitation in 2018 in wide areas of Germany influenced the management decisions to some extent and might have led to an overall decrease in mowing frequency. As the date of the first mowing event is linked to the start of the phenological season, years with an earlier start of season are expected to show earlier mowing events. Accordingly, the regionalized analyses revealed that in most federal states fewer mowing events were detected in 2018, as well as earlier dates of the first cut in comparison to 2019. While 2018, 2019 and 2020 were in general comparably warm years, 2018 was rather cold during March and overall way too dry (DWD, 2018, 2019, 2020). This caused a delayed plant development that was, however, mitigated by beneficial meteorological conditions in April, leading to phenophases being reached earlier than on long-term average (BMEL, 2018). This development was also confirmed in a remote sensing-based analysis with spring vegetation development in 2018 being above long-term average, followed by strongly negative deviations from typical phenology in summer and autumn (Reinermann et al., 2019). Even though our results reveal less intensive grassland-use patterns in 2018, we do not claim that these are caused by the abnormal drought conditions only. Confounding factors on grassland management or indirect impacts from the drought, such as economic decisions related to land management, may play an important role as well. Still, with the meteorological conditions in the years under consideration we covered extreme gradients that future climate change may enforce more often on temperate grasslands and our results highlight the robustness of the proposed approach, making it transferable to other temperate regions with similar grassland management practices if enough clear sky observations are available.

For a fair comparison throughout the years, we used a stable grassland mask and only included areas that were classified as grassland throughout the years 2017–2019. However, fodder grasses on arable land and permanent grasslands were not differentiated in their analyses and they did not consider peatlands during their mapping efforts, leading to approximately 7500 km² of permanent grasslands that we miss according to the agricultural statistics (BLE, 2021). Nevertheless, the derived maps allow to observe changes in management intensity between different years for at least 85% of the reported grassland areas in Germany.

5. Conclusions

We present a novel mowing detection algorithm that makes use of a harmonized time series of all available Sentinel-2 and Landsat 8 data. By using adaptive thresholds, the proposed algorithm accounts for variations in land surface phenology and partly for variations in data availability. The workflow was developed on an optimized ARD cube structure and performs very well without any kind of training data on a vegetation index time series. This enables transferring the approach in space and time and allows to create spatially explicit, wall-to-wall maps of temperate grassland management in a frequent manner. On this basis, we mapped the spatial distribution of grassland-use intensity for Germany for four years with a spatial resolution of 10 m × 10 m. The strong regional gradients in environmental conditions and the extreme annual variations in the meteorological conditions in the considered study area

and period, highlighted the transferability of the approach. We revealed the geographical distribution of grassland-use intensity throughout Germany and identified potential influences of extreme meteorological conditions on management decisions. In our study, meadow and pasture management intensity was not assessed independently. Since the management intensities of these two uses are accompanied by different effects, future studies should continue to aim at evaluating both grassland types separately, for which additional reference data are crucial. We showed that currently available optical time series are an important prerequisite for a reliable assessment of the intensity of grassland use. Future satellite missions should thus aim to maintain or even improve data continuity to enable long-term monitoring of land use and management in agricultural areas with high precision and frequency. This is critical, as long-term monitoring supports framework conventions and strategies at national, European, and global level that aim at the sustainable management of resources for the effective and long-term containment of climate change impacts. However, in regions that are often covered by clouds, the use of optical data may always be hampered. Thus, future mapping and monitoring attempts should further investigate the potential to integrate radar data in the analysis. The algorithm used is available as a user-defined function in the FORCE processing environment (<https://github.com/davidfrantz/force-udf/tree/main/python/ts/mowingDetection>) and all maps are online available under: <https://doi.org/10.5281/zenodo.5571613>.

Declaration of Competing Interest

The authors declare that they have no known competing financial interests or personal relationships that could have appeared to influence the work reported in this paper.

Acknowledgements

This research was part of the project SattGrün (Project No. 2818300816), which was supported by funds of the Federal Ministry of Food and Agriculture (BMEL) based on a decision of the Parliament of the Federal Republic of Germany via the Federal Office for Agriculture and Food (BLE) under the innovation support program. The authors would like to thank the associated partners of the SattGrün project Kerstin Grant (Aulendorf), Bärbel Greiner (Iden), Klaus Hünting (Kleve), Peter Kaim (Ribbeck), Christine Kalzendorf (Oldenburg), Heide Jänicke (Dummerstorf), Felix Pickert (Ramin) and Anita Styczynski (Hohenauen) for providing valuable reference data. We further thank the managers of the three Exploratories, Kirsten Reichel-Jung, Iris Steitz, Sandra Weithmann, Florian Staub, Juliane Vogt, Anna K. Franke, Miriam Teuscher and all former managers for their work in maintaining the plot and project infrastructure; Christiane Fischer and Victoria Griebmeier for giving support through the central office, Andreas Ostrowski for managing the central data base, and Markus Fischer, Eduard Linsenmair, Dominik Hessenmöller, Daniel Prati, Ingo Schöning, François Buscot, Ernst-Detlef Schulze, Wolfgang W. Weisser and the late Elisabeth Kalko for their role in setting up the Biodiversity Exploratories project. We thank the administration of the Hainich national park, the UNESCO Biosphere Reserve Swabian Alb and the UNESCO Biosphere Reserve Schorfheide-Chorin as well as all land owners for the excellent collaboration. The work has been (partly) funded by the DFG Priority Program 1374 “Biodiversity- Exploratories” (DFG-Refno.). Field work permits were issued by the responsible state environmental offices of Baden-Württemberg, Thüringen, and Brandenburg. This study contributes to the Landsat Science Team (<https://www.usgs.gov/core-science-systems/nli/landsat/2018-2023-landsat-science-team>). We thank Alice Künzel and Felix Lobert for their support with the digitization of mowing events and Planet for providing us with high-resolution data through their Education and Research Program. Further we would like to thank two anonymous reviewers that helped to improve the manuscript with valuable comments and suggestions.

Appendix A. Supplementary data

Supplementary data to this article can be found online at <https://doi.org/10.1016/j.rse.2021.112795>.

References

- Ali, I., Cawkwell, F., Dwyer, E., Barrett, B., Green, S., 2016. Satellite remote sensing of grasslands: from observation to management. *J. Plant Ecol.* 9, 649–671.
- Allan, E., Bossdorf, O., Dormann, C.F., Prati, D., Gossner, M.M., Tschardt, T., Blüthgen, N., Bellach, M., Birkhofer, K., Boch, S., Böhm, S., Börschig, C., Chazhinotas, A., Christ, S., Daniel, R., Diekötter, T., Fischer, C., Friedl, T., Glaser, K., Hallmann, C., Hodac, L., Hölzel, N., Jung, K., Klein, A.M., Klaus, V.H., Kleinebecker, T., Krauss, J., Lange, M., Morris, E.K., Müller, J., Nacke, H., Pašalić, E., Rillig, M.C., Rothenwöhrer, C., Schall, P., Scherber, C., Schulze, W., Socher, S.A., Steckel, J., Steffan-Dewenter, I., Türke, M., Weiner, C.N., Werner, M., Westphal, C., Wolters, V., Wubet, T., Gockel, S., Gorko, M., Hemp, A., Renner, S.C., Schöning, I., Pfeiffer, S., König-Ries, B., Buscot, F., Linsenmair, K.E., Schulze, E.-D., Weisser, W. W., Fischer, M., 2014. Interannual variation in land-use intensity enhances grassland multidiversity. *Proc. Natl. Acad. Sci.* 111, 308–313.
- Barsi, J.A., Alhammoud, B., Czaplina-Myers, J., Gascon, F., Haque, M.O., Kaewmanee, M., Leigh, L., Markham, B.L., 2018. Sentinel-2A MSI and Landsat-8 OLI radiometric cross comparison over desert sites. *Eur. J. Remote Sens.* 51, 822–837.
- Bastin, G., Denham, R., Scarth, P., Sparrow, A., Chewings, V., 2014. Remotely-sensed analysis of ground-cover change in Queensland's rangelands, 1988–2005. *Rangeland J.* 36, 191–204.
- Beierkuhnlein, C., 2017. Die Physische Geographie Deutschlands. WBG, Darmstadt.
- BLE, 2021. Federal Office for Agriculture and Food (BLE) and Federal Ministry of Food and Agriculture (BMEL), Statistisches Jahrbuch über Ernährung Landwirtschaft und Forsten (various years; in German only). Data source. Federal Statistical Office of Germany.
- Blickensdörfer, L., Schwieder, M., Pflugmacher, D., Nendel, C., Erasm, S., Hostert, P., 2021. National-Scale Crop Type Maps for Germany from Combined Time Series of Sentinel-1, Sentinel-2 and Landsat 8 Data (2017, 2018 and 2019). Online available. <https://doi.org/10.5281/zenodo.5153047>.
- BMEL, 2018. Federal Ministry of Food and Agriculture. Ernte 2018. Mengen und Preise (in German only). Published by Federal Ministry of Food and Agriculture. In: Buchner, J., Yin, H., Frantz, D., Kuemmerle, T., Askerov, E., Bakuradze, T., Bleyhl, B., Elizbarashvili, N., Komarova, A., Lewińska, K.E., Rizayeva, A., Sayadyan, H., Tan, B., Tepanosyan, G., Zazanashvili, N., Radeloff, V.C., 2020. Land-cover change in the Caucasus Mountains since 1987 based on the topographic correction of multi-temporal Landsat composites. *Remote Sens. Environ.* 248, 111967.
- Claverie, M., Ju, J., Masek, J.G., Dungan, J.L., Vermote, E.F., Roger, J.-C., Skakun, S.V., Justice, C., 2018. The Harmonized Landsat and Sentinel-2 surface reflectance data set. *Remote Sens. Environ.* 219, 145–161.
- De Vroey, M., Radoux, J., Defourny, P., 2021. Grassland mowing detection using Sentinel-1 time series: potential and limitations. *Remote Sens.* 13, 348.
- Destatis, 2019a. Statistisches Bundesamt. Durchschnittliche genutzte landwirtschaftliche Fläche pro Betrieb nach Bundesland in Deutschland 2019 (in Hektar). Statista GmbH. Last accessed: 17/06/2021. <https://de.statista.com/statistik/daten/studie/173089/umfrage/betriebsgroesse-von-agrarbetrieben-2010/>.
- Destatis, 2019b. Statistisches Bundesamt. Land- und Forstwirtschaft, Fischerei. Bodenfläche nach Art der tatsächlichen Nutzung. Fachserie 3 Reihe 5.1.
- Drusch, M., Del Bello, U., Carlier, S., Colin, O., Fernandez, V., Gascon, F., Hoersch, B., Isola, C., Laberinti, P., Martimort, P., Meygret, A., Spoto, F., Sy, O., Marchese, F., Bargellini, P., 2012. Sentinel-2: ESA's optical high-resolution mission for GMES operational services. *Remote Sens. Environ.* 120, 25–36.
- DWD, 2017. Deutscher Wetter Dienst. Deutschlandwetter im Jahr 2017. Press release (in German).
- DWD, 2018. Deutscher Wetter Dienst. Deutschlandwetter im Jahr 2018. Press release (in German).
- DWD, 2019. Deutscher Wetter Dienst. Deutschlandwetter im Jahr 2019. Press release (in German).
- DWD, 2020. Deutscher Wetter Dienst. Deutschlandwetter im Jahr 2020. Press release (in German).
- Dwyer, J.L., Roy, D.P., Sauer, B., Jenkerson, C.B., Zhang, H.K., Lymburner, L., 2018. Analysis ready data: enabling analysis of the Landsat archive. *Remote Sens.* 10, 1363.
- EC, 2018. (European Commission) Directorate-General for Agriculture and Rural Development. CAP explained. Direct Payments for Farmers 2015-2020.
- Fischer, M., Bossdorf, O., Gockel, S., Hänsel, F., Hemp, A., Hessenmöller, D., Korte, G., Nieschulze, J., Pfeiffer, S., Prati, D., 2010. Implementing large-scale and long-term functional biodiversity research: the biodiversity exploratories. *Basic Appl. Ecol.* 11, 473–485.
- Franke, J., Keuck, V., Siegert, F., 2012. Assessment of grassland use intensity by remote sensing to support conservation schemes. *J. Nat. Conserv.* 20, 125–134.
- Frantz, D., 2019. FORCE—Landsat + Sentinel-2 analysis ready data and beyond. *Remote Sens.* 11, 1124.
- Frantz, D., Röder, A., Stellmes, M., Hill, J., 2016a. An operational radiometric landsat preprocessing framework for large-area time series applications. *IEEE Trans. Geosci. Remote Sens.* 54, 3928–3943.
- Frantz, D., Röder, A., Udelhoven, T., Schmidt, M., 2016b. Forest disturbance mapping using dense synthetic Landsat/MODIS time-series and permutation-based disturbance index detection. *Remote Sens.* 8, 277.
- Frantz, D., Haß, E., Uhl, A., Stoffels, J., Hill, J., 2018. Improvement of the Fmask algorithm for Sentinel-2 images: separating clouds from bright surfaces based on parallax effects. *Remote Sens. Environ.* 215, 471–481.
- Gibson, D.J., Newman, J.A., 2019. Grasslands and climate change: an overview. In: Gibson, D.J., Newman, J.A. (Eds.), *Grasslands and Climate Change*. Cambridge University Press, Cambridge, pp. 3–18.
- Gómez Giménez, M., de Jong, R., Della Peruta, R., Keller, A., Schaepman, M.E., 2017. Determination of grassland use intensity based on multi-temporal remote sensing data and ecological indicators. *Remote Sens. Environ.* 198, 126–139.
- Gorelick, N., Hancher, M., Dixon, M., Ilyushchenko, S., Thau, D., Moore, R., 2017. Google earth engine: planetary-scale geospatial analysis for everyone. *Remote Sens. Environ.* 202, 18–27.
- Griffiths, P., Nendel, C., Pickert, J., Hostert, P., 2020. Towards national-scale characterization of grassland use intensity from integrated Sentinel-2 and Landsat time series. *Remote Sens. Environ.* 238, 111124.
- Helder, D., Markham, B., Morfitt, R., Storey, J., Barsi, J., Gascon, F., Clerc, S., LaFrance, B., Masek, J., Roy, D.P., Lewis, A., Pahlevan, N., 2018. Observations and Recommendations for the Calibration of Landsat 8 OLI and Sentinel 2 MSI for Improved Data Interoperability. *Remote Sensing* 10, 1340.
- Houborg, R., McCabe, M.F., 2016. High-Resolution NDVI from Planet's Constellation of Earth Observing Nano-Satellites: A New Data Source for Precision Agriculture. *Remote Sensing* 8, 768.
- Houborg, R., McCabe, M.F., 2018. A Cubesat enabled Spatio-Temporal Enhancement Method (CESTEM) utilizing Planet, Landsat and MODIS data. *Remote Sensing of Environment* 209, 211–226.
- Huete, A., Didan, K., Miura, T., Rodriguez, E.P., Gao, X., Ferreira, L.G., 2002. Overview of the radiometric and biophysical performance of the MODIS vegetation indices. *Remote Sens. Environ.* 83, 195–213.
- Huyghe, C., De Vlieghe, A., Van Gils, B., Peeters, A., 2014. *Grasslands and herbivore production in Europe and effects of common policies*. éditions Quae 320. <https://doi.org/10.35690/978-2-7592-2157-8>.
- Imbery, F., Kaspar, F., Friedrich, K., Plüchhahn, B., 2021. Klimatologischer Rückblick auf 2020: Eines der Wärmsten Jahre in Deutschland und Ende des Bisher Wärmsten Jahrzehnts. Deutscher Wetterdienst - Abteilungen für Klimaüberwachung und Agrarmeteorologie.
- Jakimov, B., van der Linden, S., Thiel, F., Frantz, D., Hostert, P., 2020. Visualizing and labeling dense multi-sensor earth observation time series: the EO time series viewer. *Environ. Model. Softw.* 125, 104631.
- Klein, N., Theux, C., Arletaz, R., Jacot, A., Pradervand, J.-N., 2020. Modeling the effects of grassland management intensity on biodiversity. *Ecol. Evol.* 10, 13518–13529.
- Kolecak, N., Ginzler, C., Pazur, R., Price, B., Verburg, P., 2018. Regional scale mapping of grassland mowing frequency with Sentinel-2 time series. *Remote Sens.* 10, 1221.
- Le Clec'h, S., Finger, R., Buchmann, N., Gosal, A.S., Hörtnagl, L., Huguenin-Elie, O., Jeanneret, P., Lüscher, A., Schneider, M.K., Huber, R., 2019. Assessment of spatial variability of multiple ecosystem services in grasslands of different intensities. *J. Environ. Manag.* 251, 109372.
- Lewińska, K.E., Hostert, P., Buchner, J., Bleyhl, B., Radeloff, V.C., 2020. Short-term vegetation loss versus decadal degradation of grasslands in the Caucasus based on Cumulative Endmember fractions. *Remote Sens. Environ.* 248, 111969.
- Lewis, A., Oliver, S., Lymburner, L., Evans, B., Wyborn, L., Mueller, N., Raevksi, G., Hooke, J., Woodcock, R., Sixsmith, J., Wu, W., Tan, P., Li, F., Killough, B., Minchin, S., Roberts, D., Ayers, D., Bala, B., Dwyer, J., Dekker, A., Dhu, T., Hicks, A., Ip, A., Purss, M., Richards, C., Sagar, S., Trenham, C., Wang, P., Wang, L.-W., 2017. The Australian geoscience data cube — foundations and lessons learned. *Remote Sens. Environ.* 202, 276–292.
- Loberf, F., Holtgrave, A.-K., Schwieder, M., Pause, M., Vogt, J., Gocht, A., Erasm, S., 2021. Mowing event detection in permanent grasslands: systematic evaluation of input features from Sentinel-1, Sentinel-2, and Landsat 8 time series. *Remote Sens. Environ.* 267, 112751.
- Mielke, H., Wohlers, W., 2019. *Praxishandbuch Grünland: Nutzung und Pflege*, (2. ed.). Agrimedia.
- Munyati, C., Makgale, D., 2009. Multitemporal Landsat TM imagery analysis for mapping and quantifying degraded rangeland in the Bahurutshe communal grazing lands, South Africa. *Int. J. Remote Sens.* 30, 3649–3668.
- Planet Team, 2017. Planet Application Program Interface. In *Space for Life on Earth*, San Francisco, CA. <https://api.planet.com>.
- Qiu, S., Zhu, Z., He, B., 2019. Fmask 4.0: improved cloud and cloud shadow detection in Landsats 4–8 and Sentinel-2 imagery. *Remote Sens. Environ.* 231, 111205.
- Reinermann, S., Gessner, U., Asam, S., Kuenzer, C., Dech, S., 2019. The effect of droughts on vegetation condition in Germany: an analysis based on two decades of satellite earth observation time series and crop yield statistics. *Remote Sens.* 11, 1783.
- Reinermann, S., Asam, S., Kuenzer, C., 2020. Remote sensing of grassland production and management—a review. *Remote Sens.* 12, 1949.
- Roy, D.P., Li, Z., Zhang, H.K., 2017. Adjustment of Sentinel-2 multi-spectral instrument (MSI) red-edge band reflectance to Nadir BRDF adjusted reflectance (NBAR) and quantification of red-edge band BRDF effects. *Remote Sens.* 9, 1325.
- Rufin, P., Frantz, D., Yan, L., Hostert, P., 2021. Operational coregistration of the Sentinel-2A/B image archive using multitemporal landsat spectral averages. *IEEE Geosci. Remote Sens. Lett.* 1–5.
- Sadeh, Y., Zhu, X., Dunkerley, D., Walker, J.P., Zhang, Y., Rozenstein, O., Manivasagam, V.S., Chen, K., 2021. Fusion of Sentinel-2 and PlanetScope time-series data into daily 3 m surface reflectance and wheat LAI monitoring. *International Journal of Applied Earth Observation and Geoinformation* 96, 102260.
- Scheffler, D., Frantz, D., Segl, K., 2020. Spectral harmonization and red edge prediction of Landsat-8 to Sentinel-2 using land cover optimized multivariate regressors. *Remote Sens. Environ.* 241, 111723.

- Schwieder, M., Frantz, D., Loibl, D., Griffiths, P., Pfoch, K., Lilienthal, H., Hostert, P., 2019. Grassland Use Intensity Metrics from Sentinel-1 and Sentinel-2 Data. ESA Living Planet Symposium Milan, Italy.
- Skakun, S., Vermote, E.F., Roger, J., Justice, C.O., Masek, J.G., 2019. Validation of the LaSRC cloud detection algorithm for Landsat 8 images. *IEEE J. Select. Top. Appl. Earth Observ. Remote Sens.* 1–8.
- Smit, H.J., Metzger, M.J., Ewert, F., 2008. Spatial distribution of grassland productivity and land use in Europe. *Agric. Syst.* 98, 208–219.
- Sokolova, M., Japkowicz, N., Szpakowicz, S., 2006. Beyond accuracy, F-score and ROC: A family of discriminant measures for performance evaluation. In: *AI 2006: Advances in Artificial Intelligence*. Springer, Berlin, Heidelberg, Germany, pp. 1015–1021.
- Stumpf, F., Schneider, M.K., Keller, A., Mayr, A., Rentschler, T., Meuli, R.G., Schaepman, M., Liebisch, F., 2020. Spatial monitoring of grassland management using multi-temporal satellite imagery. *Ecol. Indic.* 113, 106201.
- Tamm, T., Zalite, K., Voormansik, K., Talgre, L., 2016. Relating Sentinel-1 interferometric coherence to mowing events on grasslands. *Remote Sens.* 8.
- Taravat, A., Wagner, M.P., Oppelt, N., 2019. Automatic grassland cutting status detection in the context of spatiotemporal Sentinel-1 imagery analysis and artificial neural networks. *Remote Sens.* 11, 711.
- Tscharntke, T., Klein, A.M., Kruess, A., Steffan-Dewenter, I., Thies, C., 2005. Landscape perspectives on agricultural intensification and biodiversity–ecosystem service management. *Ecol. Lett.* 8, 857–874.
- USGS, 2021. Landsat Collection 2 (ver. 1.1, January 15, 2021). In: (p. 4). U.S. Geological Survey Fact Sheet 2021–3002. US Geological Survey.
- Vogt, J., Klaus, V.H., Both, S., Fürstenau, C., Gockel, S., Gossner, M.M., Heinze, J., Hemp, A., Hölzel, N., Jung, K., Kleinebecker, T., Lauterbach, R., Lorenzen, K., Ostrowski, A., Otto, N., Prati, D., Renner, S., Schumacher, U., Seibold, S., Simons, N., Steitz, I., Teuscher, M., Thiele, J., Weithmann, S., Wells, K., Wiesner, K., Ayasse, M., Blüthgen, N., Fischer, M., Weisser, W.W., 2019. Eleven years' data of grassland management in Germany. *Biodivers. Data J.* 7: e36387.
- Voormansik, K., Jagdhuber, T., Zalite, K., Noorma, M., Hajnsek, I., 2016. Observations of cutting practices in agricultural grasslands using polarimetric SAR. *IEEE J. Select. Top. Appl. Earth Observ. Remote Sens.* 9, 1382–1396.
- Voormansik, K., Zalite, K., Sünter, I., Tamm, T., Koppel, K., Verro, T., Brauns, A., Jakovels, D., Praks, J., 2020. Separability of mowing and ploughing events on short temporal baseline Sentinel-1 coherence time series. *Remote Sens.* 12, 3784.
- Wesemeyer, M., Schwieder, M., Pickert, J., Hostert, P., 2021. Identifying areas of homogeneous grassland management based on iterative segmentation of Sentinel-1 and Sentinel-2 monthly composites. In: Astor, T., Dzene, I. (Eds.), *EGF 2021 Grassland Science in Europe*, Vol. 26. Universität Kassel, Germany, pp. 208–210.
- White, R.P., Murray, S., Rohweder, M., 2000. *Grassland Ecosystems*. World Resources Institute, Washington, DC, USA.
- Wrage, N., Strodthoff, J., Cuchillo, H.M., Iselstein, J., Kayser, M., 2011. Phytodiversity of temperate permanent grasslands: ecosystem services for agriculture and livestock management for diversity conservation. *Biodivers. Conserv.* 20, 3317–3339.
- Wulder, M.A., Hilker, T., White, J.C., Coops, N.C., Masek, J.G., Pflugmacher, D., Crevier, Y., 2015. Virtual constellations for global terrestrial monitoring. *Remote Sens. Environ.* 170, 62–76.
- Wulder, M.A., Coops, N.C., Roy, D.P., White, J.C., Hermosilla, T., 2018. Land cover 2.0. *Int. J. Remote Sens.* 39, 4254–4284.
- Yan, L., Roy, D.P., Li, Z., Zhang, H.K., Huang, H., 2018. Sentinel-2A multi-temporal misregistration characterization and an orbit-based sub-pixel registration methodology. *Remote Sens. Environ.* 215, 495–506.
- Zhao, Y., Liu, Z., Wu, J., 2020. Grassland ecosystem services: a systematic review of research advances and future directions. *Landsc. Ecol.* 35, 793–814.
- Zhou, W., Yang, H., Huang, L., Chen, C., Lin, X., Hu, Z., Li, J., 2017. Grassland degradation remote sensing monitoring and driving factors quantitative assessment in China from 1982 to 2010. *Ecol. Indic.* 83, 303–313.
- Zhu, Z., Woodcock, C.E., 2012. Object-based cloud and cloud shadow detection in Landsat imagery. *Remote Sens. Environ.* 118, 83–94.
- Zhu, Z., Woodcock, C.E., 2014. Continuous change detection and classification of land cover using all available Landsat data. *Remote Sens. Environ.* 144, 152–171.
- Zhu, Z., Wang, S., Woodcock, C.E., 2015. Improvement and expansion of the Fmask algorithm: cloud, cloud shadow, and snow detection for Landsats 4–7, 8, and Sentinel 2 images. *Remote Sens. Environ.* 159, 269–277.
- Zhu, Z., Zhang, J., Yang, Z., Aljaddani, A.H., Cohen, W.B., Qiu, S., Zhou, C., 2020. Continuous monitoring of land disturbance based on Landsat time series. *Remote Sens. Environ.* 238, 111116.